Electronic Supplementary Material (ESI) for CrystEngComm.

Supporting Information

Locked guest PAHs by soft−cavity−type host assembled via halogen bond to form luminescence cocrystals

Wen Xin Wu,[a] *Hui Wang*,*[b] *Wei Jun Jin**[a]

[a]College of Chemistry, Beijing Normal University, Beijing, 100875, People's Republic of China

[b]College of Chemistry & Material Science, Shanxi Normal University, Linfen, Shanxi, 041004, People's Republic of China

Correspondence email: wanghui@sxnu.edu.cn, wjjin@bnu.edu.cn

PART I. Crystallography data and crystal structures

PART II. Hirshfeld surface analysis

PART III. Molecular surface electrostatic potential

PART IV. Phosphorescence studies

PART I. Crystallography data and crystal structures

Cocrystal **Host:** *1,4−DITFB:PPNO (2:1)*

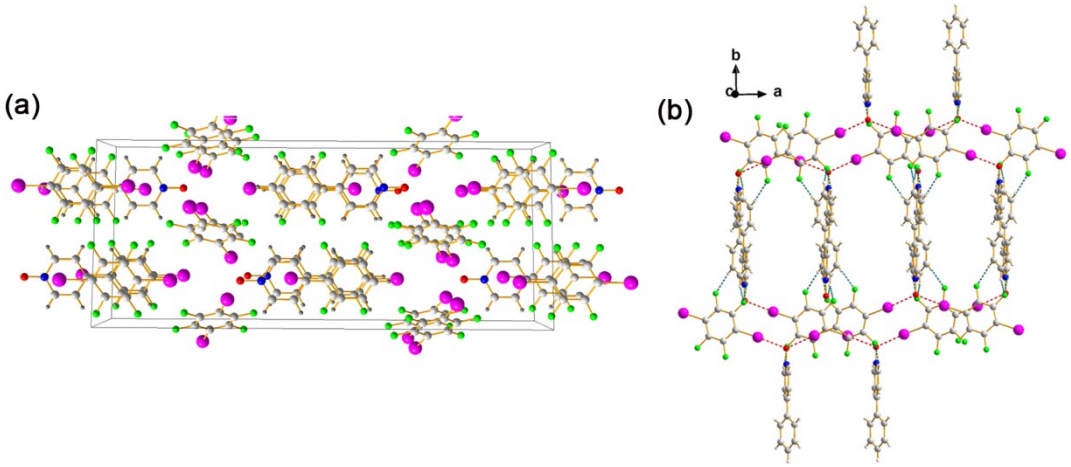

Fig. S1 Structural details of cocrystal **Host**: (a) The crystal cell unit. (b) Ball and stick model of 3D supermolecular cavity structure constructed by C−I···$^{-}$O−N^{+} and C−H···F bonds along *c*−axis.

The binary cocrystal **Host** possesses the space group monoclinic with *Z*=4, *cf*. **Table 1**. The asymmetric unit has two independent 1,4−DITFB molecules and one independent PPNO molecule with no imposed symmetry.

Cocrystal **HPyr:** *1,4−DITFB:PPNO:Pyr (2:2:1)*

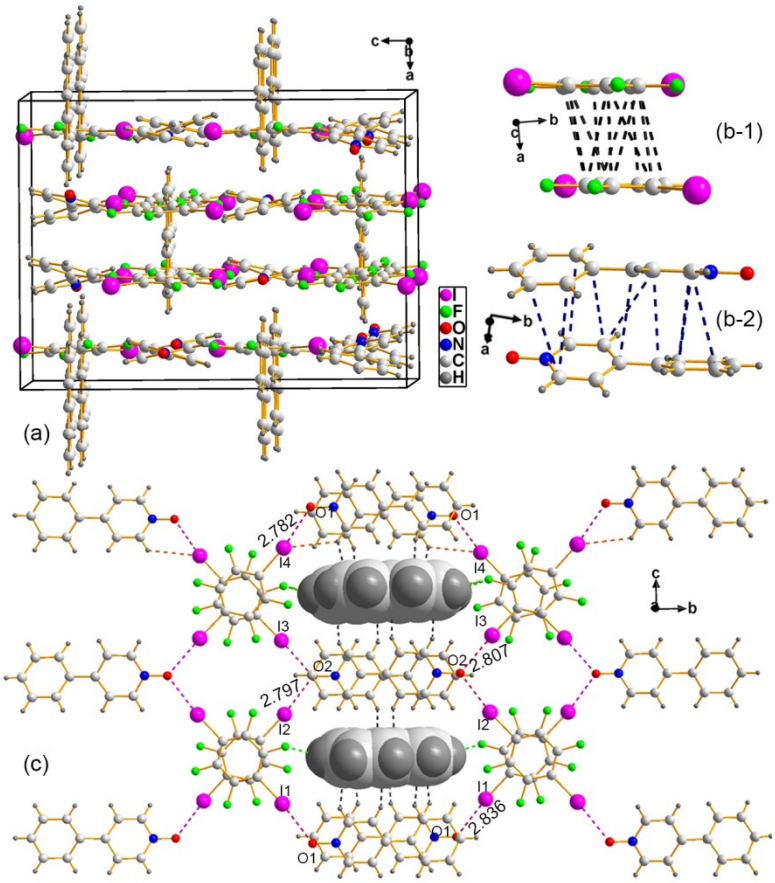

Fig. S2 Structural details of **HPyr**: (a) The crystal cell unit. (b−1) and (b−2) the π−hole···π−hole bonds of crossed 1,4−DITFBs between adjacent layers and the π−hole···π stacking of two reversed PPNOs. (c) The host−guest structural units extended to *a*−axis with reversed Pyr molecules trapped in the cavities by C−H···F and C−H···π bonds.

The ternary host−guest cocrystal **HPyr** possesses the space group orthorhomibic with *Z*=4, *cf*. **Table 1**. The asymmetric unit has two independent 1,4−DITFB molecules, two independent PPNO molecules, and one independent Pyr molecules with no imposed symmetry. (distance in Å).

Cocrystal **HTph:** *1,4−DITFB:PPNO:Tph (2:2:1)*

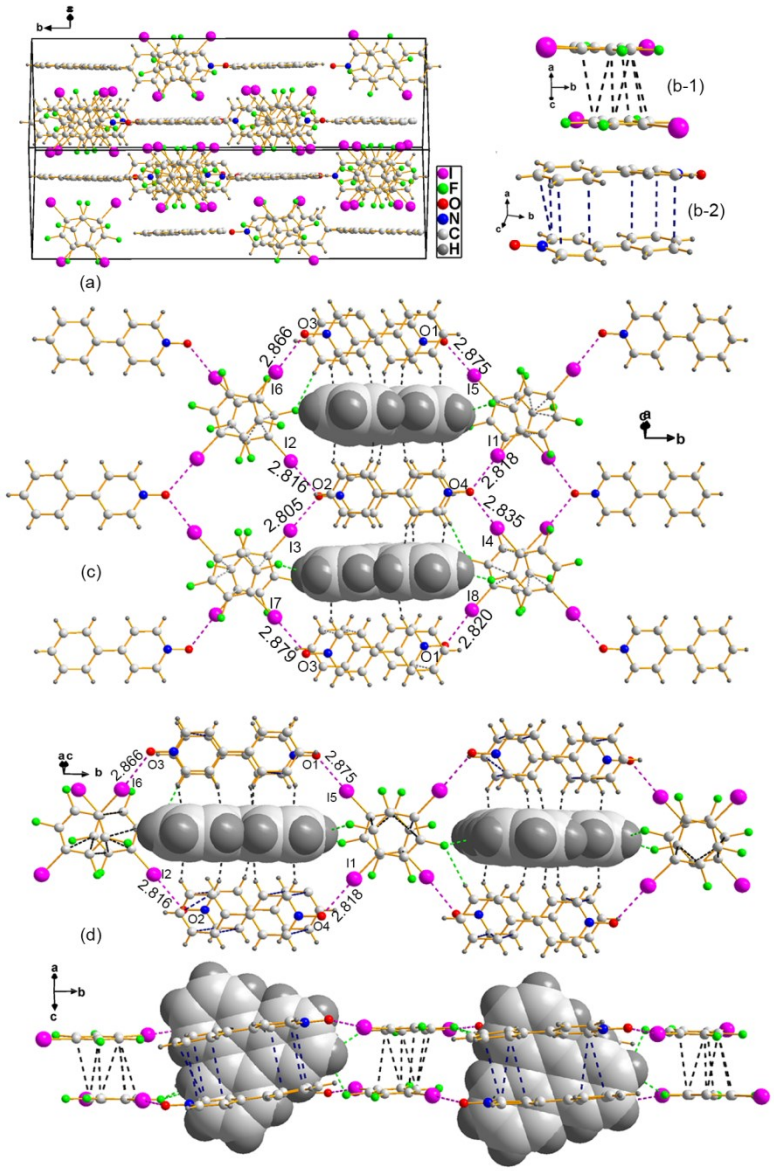

Fig. S3 Structural details of **HTph**: (a) The crystal cell unit. (b−1) and (b−2) the π−hole···π−hole bonds of crossed 1,4−DITFBs between adjacent layers and the π−hole···π stacking of two reversed PPNOs. (c) The host−guest structural units extended to *o*−axis with reversed Tph molecules trapped in the cavities by C−H···F and C−H···π bonds. (d) Top view and side view of extracted 3D supermolecular host−guest units with reversed Tph molecules trapped in the cavity by C−H···F and C−H···π bonds (distance in Å).

The ternary host−guest cocrystal **HTph** possesses the space group monoclinic with *Z*=4, *cf*. **Table 1**. The asymmetric unit has four independent 1,4−DITFB molecules, four independent PPNO molecules, and two independent Tph molecules with no imposed symmetry.

Cocrystal **HFan:** *1,4−DITFB:PPNO:Fan (2:2:1)*

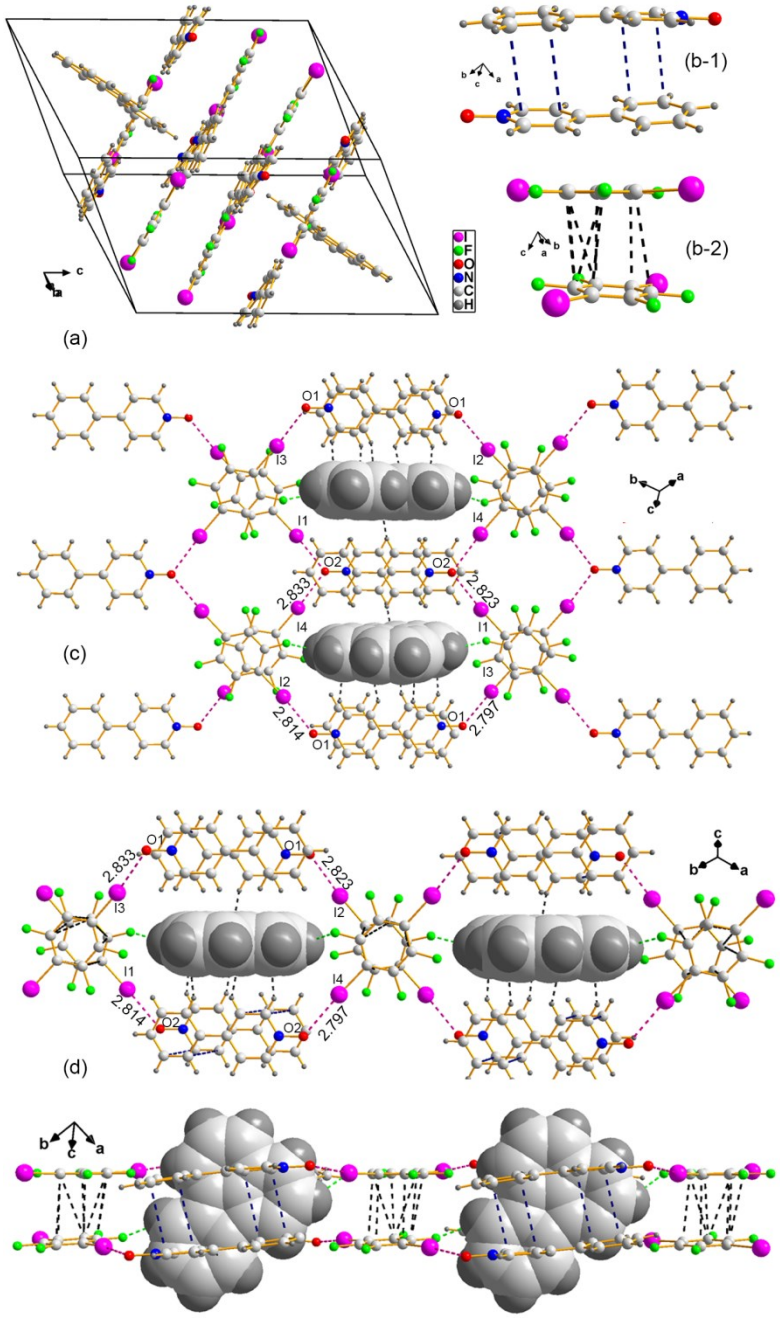

Fig. S4 Structural details of **HFan**: (a) The crystal cell unit. (b−1) and (b−2) The π−hole···π stacking of two reversed PPNOs and the π−hole···π−hole bonds of crossed 1,4−DITFBs between adjacent layers. (c) The host−guest structural units extended to *o*−axis with reversed Fan molecules trapped in the cavities by C−H···F and C−H···π bonds. (d) Top view and side view of extracted 3D supermolecular host−guest units with reversed Fan molecules trapped in the cavity by C−H···F and C−H···π bonds

(distance in Å).

The ternary host–guest cocrystal **HFan** possesses the space group triclinic with Z=2, *cf*. **Table 1**. The asymmetric unit has two independent 1,4–DITFB molecules, two independent PPNO molecules, and one independent Fan with no imposed symmetry.

Cocrystal **HPer:** *1,4−DITFB:PPNO:Per (3:3:2)*

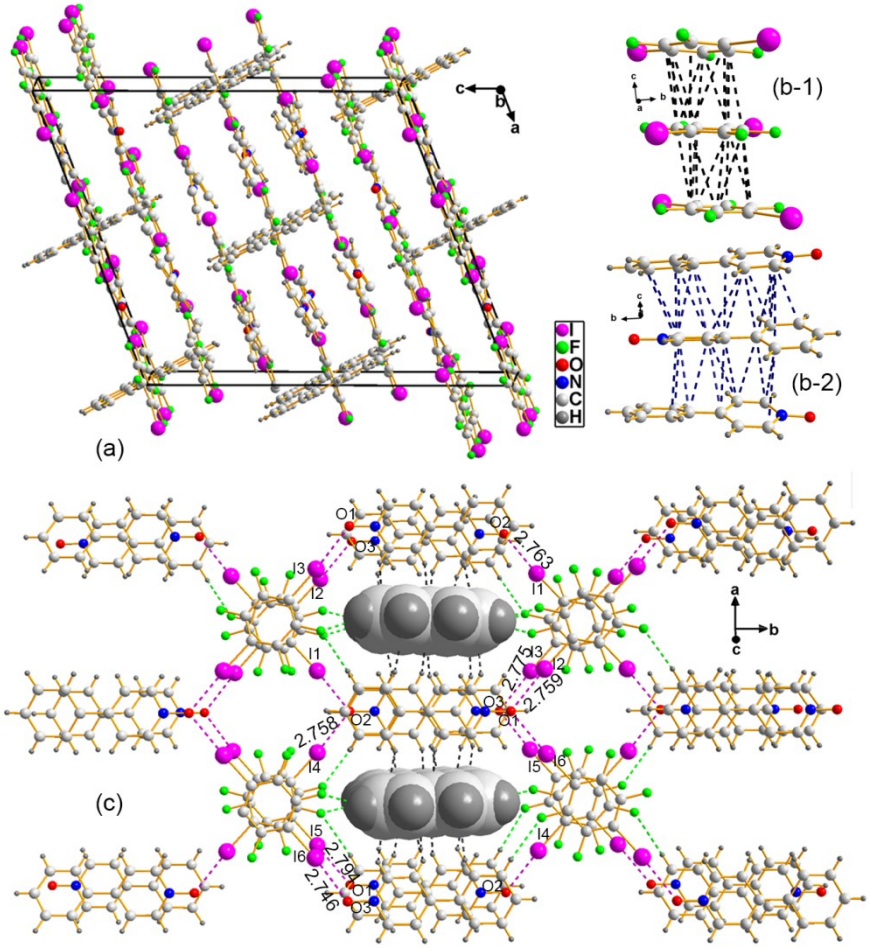

Fig. S5 Structural details of **HPer**: (a) The crystal cell unit. (b−1) and (b−2) the π−hole···π−hole···π−hole bonds of three crossed 1,4−DITFBs from adjacent three layers and the π−hole···π···π−hole stacking of three oppositely aligned PPNOs. (c) The host−guest structural units extended to *o*−axis with reversed Fan molecules trapped in the cavities by C−H···F and C−H···π bonds.

The ternary host−guest cocrystal **HPer** possesses the space group monoclinic with *Z*=4, *cf*. **Table 1**. The asymmetric unit has three independent 1,4−DITFB molecules, three independent PPNO molecule, and one independent Per with no imposed symmetry.

Cocrystal **HBaA:** *1,4−DITFB:PPNO:BaA (3:3:2)*

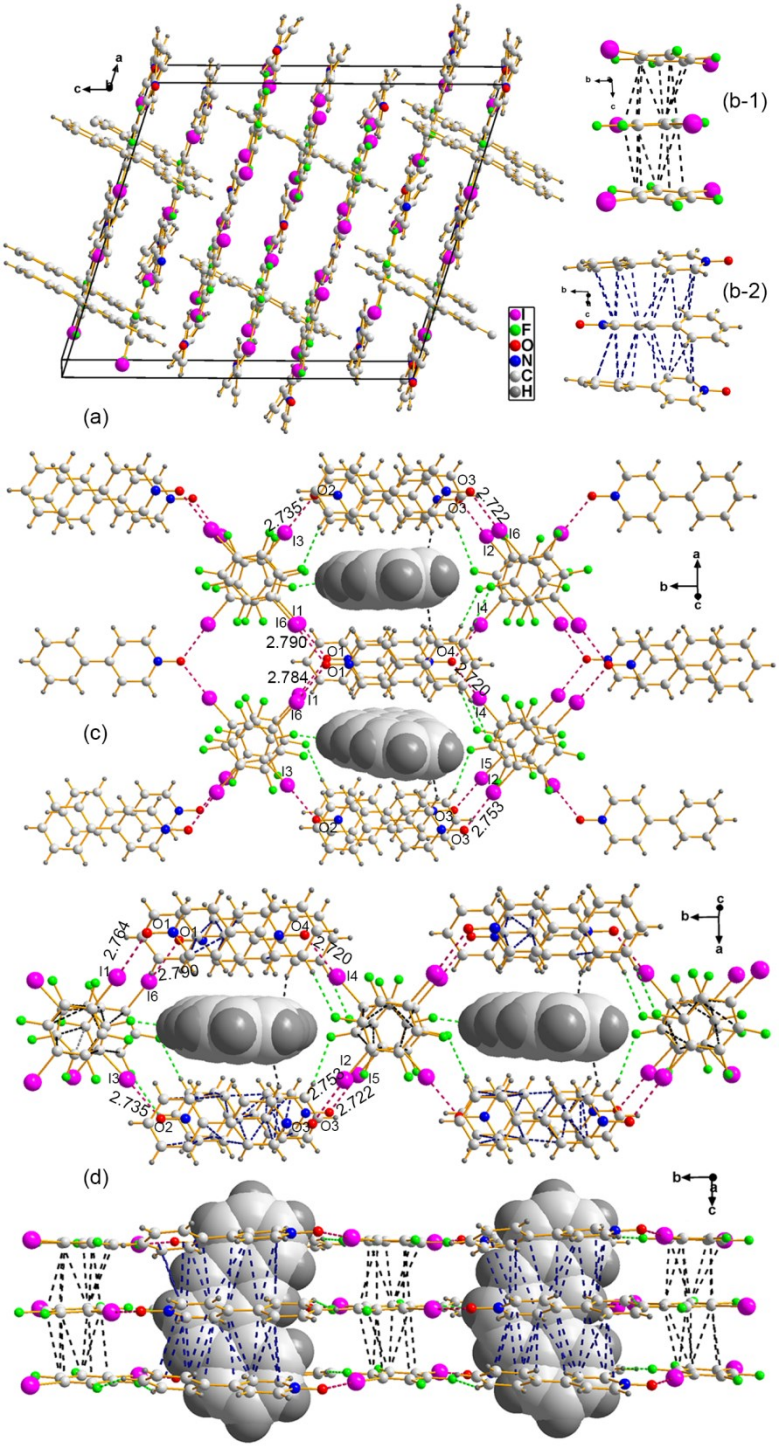

Fig. S6 Structural details of **HBaA**: (a) The crystal cell unit. (b−1) and (b−2) the π–hole···π–hole···π–hole bonds of three crossed 1,4−DITFBs from adjacent three layers and the π−hole···π···π−hole stacking of three oppositely aligned PPNOs. (c) The host−guest structural units extended to *c*−axis with reversed BaA molecules trapped in

the cavity by C–H···F and C–H···π bonds. (d) Top view and side view of extracted 3D supermolecular host−guest units with reversed BaA molecules trapped in the cavity by C–H···F and C–H···π bonds (distance in Å).

The ternary cocrystal **HBaA** possesses the space group monoclinic with *Z*=4, *cf*. **Table 1**. The asymmetric unit has three independent 1,4−DITFB molecules, three independent PPNO molecules, and one independent BaA with no imposed symmetry

Table S1 Interactions and geometrical parameters in the cocrystals

Cocrystals	Interactions	*d*/Å	*θ*/°
Host	C1−I3···O1−N1	2.7616(10) (−21.10%)	176.8(9)
	C8−H8···F4	2.475 (−7.30%)	159.44
	C12−H12···F1	2.346 (−12.13%)	167.70
	C13−H13···F3	2.530 (−5.24%)	169.59
	C14−H14···F4	2.636 (−1.27%)	118.41
	C5−I3···N1	3.463 (−1.90%)	156.13
HPyr	C−I3···O2−N2	2.807(3) (−19.80%)	175.5(2)
	C−I2···O2−N2	2.797(4) (−20.08%)	171.0(19)
	C−I4···O1−N1	2.782(4) (−20.51%)	171.0(17)
	C−I1···O1−N1	2.836(3) (−18.97%)	174.0(17)
	C−I4···H13	3.095 (−2.8%)	138.18
	C−H36···F8	2.530 (−5.13%)	122.79
	C−H35···F8	2.589 (−1.67%)	120.27
	C−H44···F1	2.543 (−4.34%)	160.96
	C−C36···F8	3.133 (−1.26%)	158.06
	C−C35···F8	3.161 (−0.6%)	159.83
	C−H25···π	2.819 (−7.57%)	82.55
	C−H26···π	2.818 (−7.61%)	82.05
	C−H27···π	2.839 (−6.91%)	58.77
	C−H14···π	2.871 (−5.87%)	78.99
	C−H16···π	2.881 (−5.54%)	74.40
	C−H20···π	2.886(−5.38%)	78.04
	C−H13···π	2.852 (−6.49%)	76.86
	C−H19···π	2.860 (−6.23%)	78.83
HTph	C−I2···O2−N2	2.817(6) (−19.54%)	175.9(2)
	C−I3···O2−N2	2.806(5) (−19.86%)	175.4(2)
	C−I4···O4−N4	2.836(6) (−19.00%)	173.3(3)
	C−I1···O4−N4	2.817(6) (−19.49%)	173.1(3)
	C−I7···O3−N3	2.881(6) (−17.68%)	173.3(2)
	C−I6···O3−N3	2.867(6) (−18.12%)	174.7(3)
	C−I5···O1−N1	2.875(6) (−17.86%)	172.5(2)

	C−I8···O1−N1	2.821(6) (−19.44%)	173.7(2)
	C−H26···F2	2.635 (−1.20%)	171.7
	C−H45···F10	2.568 (−3.82%)	161.1
	C−H75···F12	2.554 (−4.42%)	125.3
	C−H76···F5	2.652 (−0.67%)	125.0
	C−H86···F7	2.603 (−2.28%)	140.3
	C−H90···F2	2.497 (−6.59%)	136.9
	C−H101···F14	2.632 (−1.65%)	131.6
	C−H101···F4	2.525 (−5.32%)	127.8
	C−H82···F10	2.548 (−4.87%)	161.8
	C−H80···F3	2.629 (−1.72%)	114.1
	C−H66···π	2.859 (−6.26%)	82.31
	C−H51···π	2.830 (−6.95%)	92.44
	C−H67···π	2.873 (−5.74%)	76.80
	C−H68···π	2.821 (−7.50%)	97.71
	C−H69···π	2.842 (−6.82%)	77.67
	C−H74···π	2.912 (−4.52%)	83.72
	C−H46···π	2.795 (−8.36%)	97.56
	C−H64···π	2.874 (−5.77%)	82.63
	C−H55···π	2.894 (−5.05%)	99.67
	C−H57···π	2.899 (−5.05%)	99.42
	C−H58···π	2.808 (−8.03%)	91.67
	C−H59···π	2.865 (−6.10%)	93.25
	C−H62···π	2.833 (−7.11%)	91.24
	C−H47···π	2.807 (−8.00%)	92.44
HFan	C−I1···O2−N2	2.815(3) (−19.60%)	173.2(15)
	C−I2···O1−N1	2.822(3) (−19.34%)	172.8 (15)
	C−I3···O1−N1	2.835(4) (−19.06%)	174.8(15)
	C−I4···O2−N2	2.798(4) (−20.09%)	174.0 (15)
	C−H39···F8	2.638 (−1.09%)	124.3
	C−H49···F2	2.551 (−4.42%)	135.2
	C−H14···π	2.825 (−7.25%)	86.6
	C−H16···π	2.869 (−5.93%)	76.1
	C−H19···π	2.812 (−7.80%)	93.6
	C−H15···π	2.880 (−5.41%)	86.9
	C−H13···π	2.829 (−7.34%)	94.9

	C−H31···π	2.854 (−6.46%)	89.3
3.HPer	C−I6···O3−N3	2.746(3) (−21.54%)	173.9(15)
	C−I3···O3−N3	2.775(3) (−20.71%)	175.7(14)
	C−I2···O1−N1	2.759(3) (−21.17%)	174.2(15)
	C−I5···O1−N1	2.794(3) (−20.17%)	174.7 (14)
	C−I4···O2−N2	2.758(3) (−21.20%)	175.7 (15)
	C−I1···O2−N2	2.763(3) (−21.06%)	175.1(15)
	C−H20···F5	2.522 (−5.54%)	162.9
	C−H42···F11	2.613 (−2.13%)	168.3
	C−H68···F10	2.551 (−4.46%)	131.5
	C−H63···F8	2.485 (−7.00%)	163.8
	C−H64···F11	2.439 (−8.65%)	159.9
	C−H54···F4	2.455 (−8.09%)	149.1
	C−H53···F1	2.471 (−7.45%)	164.5
	C−H20···F5	2.522 (−5.54%)	143.9
	C−H58···F5	2.448 (−8.28%)	143.8
	C−H50···I6	3.149 (−1.25%)	135.7
	C−H50···π	2.825(−7.38%)	97.4
	C−H33···π	2.858(−6.30%)	97.2
	C−H27···π	2.862(−6.16%)	85.4
	C−H44···π	2.835(−7.18%)	99.7
	C−H37···π	2.864(−6.07%)	79.3
	C−H48···π	2.875(−5.77%)	98.2
	C−H45···π	2.894(−5.05%)	89.9
	C−H22···π	2.887(−5.34%)	85.9
	C−H49···π	2.879(−5.61%)	76.9
	C−H38···π	2.884(−5.44%)	76.8
	C−H51···π	2.840(−6.81%)	87.0
	C−H28···π	2.882(−5.57%)	93.3
HBaA	C−I2···O3−N3	2.748 (−21.48%)	175.0(7)
	C−I5···O3−N3	2.718 (−22.34%)	175.8 (5)
	C−I3···O2−N2	2.733 (−21.86%)	176.7(7)
	C−I1···O1−N1	2.787 (−20.46%)	174.4(4)
	C−I4···O4−N4	2.729 (−22.86%)	175.6(5)
	C−I6···O1−N1	2.782 (−20.51%)	174.3(5)
	C−H1···F10	2.607 (−2.36%)	130.0

	C−H71···F9	2.592 (−2.66%)	158.5
	C−H14···F5	2.536 (−5.02%)	155.2
	C−H26···F2	2.547 (−4.60%)	125.8
	C−H37···F8	2.631 (−1.46%)	155.1
	C−H29···π	2.899(−4.95%)	99.6
	C−H64···π	2.894(−5.11%)	83.3

PART II. Hirshfeld surface analysis

The interactions, appearance and geometries of Pyr, Tph, Fan, Per and BaA guest molecules in host−guest ternary cocrystals were represented by means of Hirshfeld surface analysis which was carried out using Multiwfn program (version 3.7)[S1] and Mapped by the VMD program[S2].

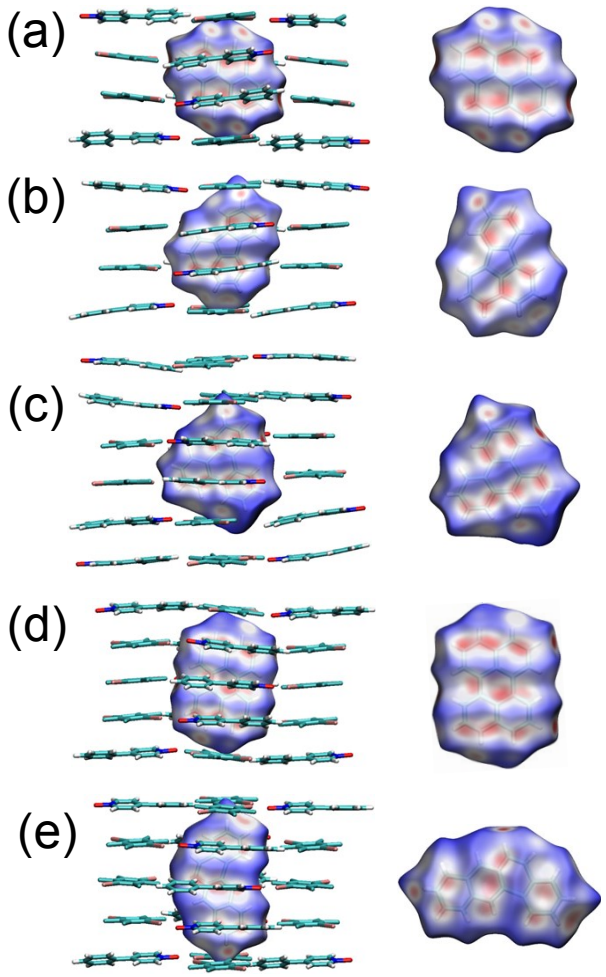

Figure S7. Hirshfeld surfaces mapped with d_{norm} for the five PAHs guest molecules extracted from host-guest ternary cocrystal. The overlapped surfaces are marked in red, touching areas are marked in white, and separated areas are marked in blue.

PART III. Molecular surface electrostatic potential

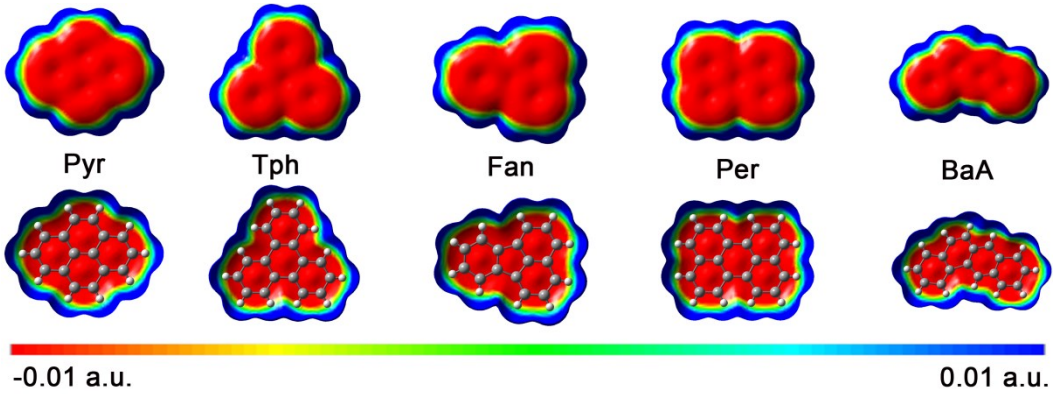

Fig. S8 Maps (electron density 0.001 $e \cdot \text{Bohr}^{-3}$) of electrostatic potential surface of guest molecules extracted from cocrystals **HPyr**, **HTph**, **HFan**, **HPer** and **HBaA** calculated at M06−2X/6−311G(d) level using GAUSSIAN 09 quantum chemistry package[S3]. Colour ranges from red to blue represents the increasing SEP from negative to positive.

PART IV. Phosphorescence studies

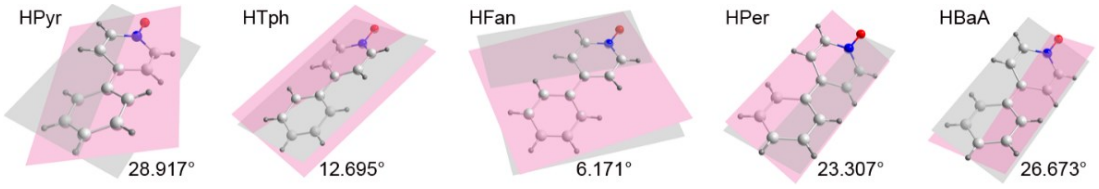

Fig. S9 Dihedral angle of PPNOs from ternary host−guest cocrystals.

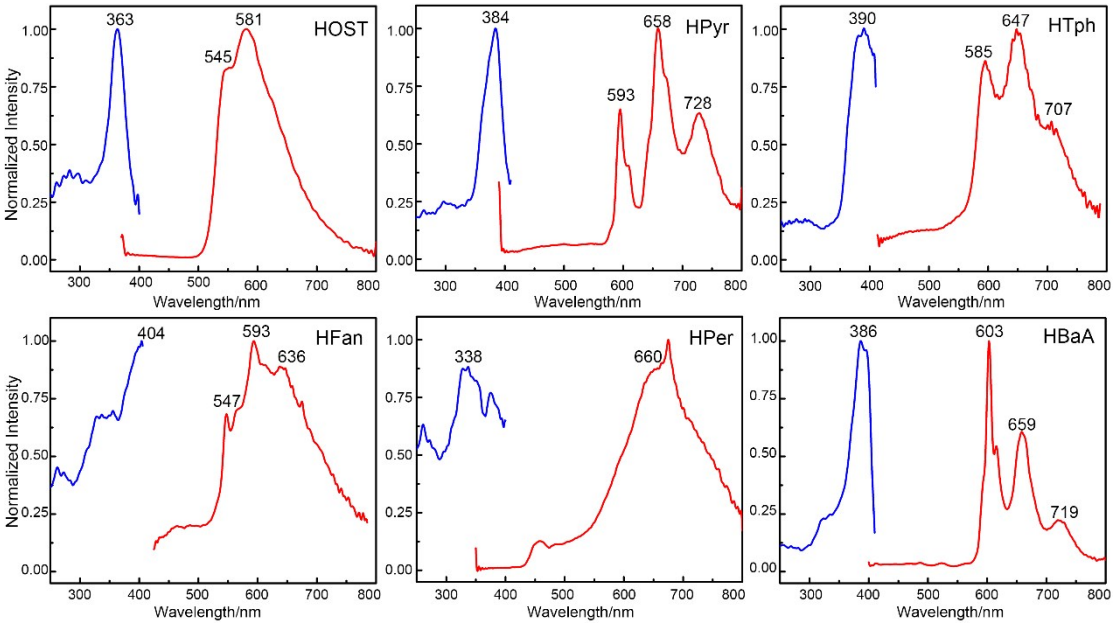

Fig. S10 The normalized phosphorescence and delayed fluorescence excitation and emission spectra of cocrystals under phosphorescence model. Excitation spectra: red lines; Emission spectra: black lines, respectively.

It is well known that PPNO has a dihedral angle of 22.568 degree in cocrystal **Host**, but it exhibits strong phosphorescence because of heavy atom effect of iodine atom and possible coplanarity in its exited state. However, PPNO molecules exist in dimer or trimer in all ternary cocrystals, so PPNO maintains silence−state of luminescence due to self−quenching. In addition, PPNO and guest molecules almost are orthogonal in all ternary cocrystals. The relative orientation is not beneficial to energy transfer or other

interaction between PPNO and guest molecules. Therefore, the luminescence from guest molecules in ternary cocrystals should be relatively independent. Fig. S10 shows the normalized phosphorescence and delayed fluorescence spectra of cocrystals. Cocrystal **Host** under both fluorescence and phosphorescence models produces phosphorescence. The phosphorescence spectrum from ternary cocrystals locate longer wavelength region compared with cocrystal **Host**. For phosphorescence decays, **HPyr** aside by mono−exponential attenuation model with the average lifetime of 3.013 ms and **HBaA** aside by tri−exponential attenuation model with the average lifetime of 6.426 ms. Nevertheless, phosphorescence decays of cocrystal **Host, HTph**, **HFan** and **HPer** obey bi−exponential attenuation model with the average lifetime of 1.236, 0.230, 0.133 and 0.036 ms, respectively (*cf.* Table S2).

Table S2 The phosphorescent properties of ternary cocrystals

Cocrystal	Spectra/λ, nm		Decays			
	λ_{ex}	λ_{em}	$\tau_1(f_1,\%)$	$\tau_2(f_2,\%)$	$\tau_3(f_3,\%)$	τ_{ave}/ms
Host	363	545, ***581***	0.663(40.03)	81.60(59.97)	−−−	1.236
HPyr	384	593, ***658***, 728	3.013(100.00)	−−−	−−−	3.013
HTph	390	595, ***647***, 707	0.011(66.29)	0.660(33.71)	−−−	0.230
HFan	404	547, ***593***, 636	0.026(36.79)	0.196(63.21)	−−−	0.133
HPer	338	*458*, **660**	0.019(96.50)	0.500(3.50)	−−−	0.036
HBaA	386	**603**,659, 719	0.028(1.11)	2.838(32.30)	8.272(66.60)	6.426

Notes: **λ**: the maximum emission position; τ_1, τ_2 and τ_3: the lifetime of long−lived and short−lived components; f_1, f_2 and f_3: the fractional contribution of long−lived and short−lived components, ave=average.

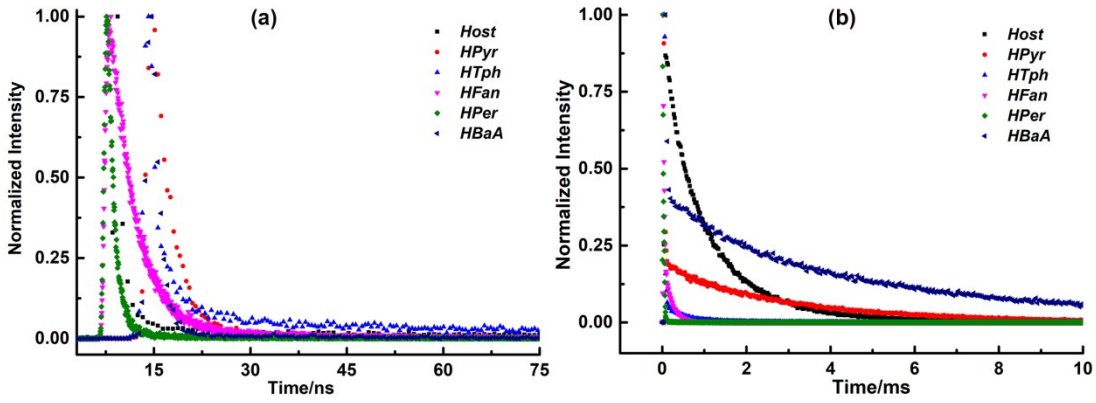

Fig. S11 Fluorescence (a) and phosphorescence (b) decay curves of all those cocrystals at their optimum emission and optimal excitation at 298 K. Luminescence lifetime of all those cocrystals were measured under optimal excitation and optimal emission condition.

Reference

[S1] Lu, T.; Chen, F. Multiwfn: A multifunctional wavefunction analyzer. *J. Comput. Chem*., 2012, **33**, 580–592.

[S2] Humphrey, W.; Dalke, A.; Schulten, K. VMD: Visual molecular dynamics. *J. Mol. Graph*., 1996, **14**, 33−38.

[S3] Frisch, M. J.; Trucks, G. W.; Schlegel, H. B.; Scuseria, G. E.; M.A. Robb, J. R.; Cheeseman, G.; Scalmani; Barone, V.; Mennucci, B.; Petersson, G. A.; Nakatsuji, H.; Caricato, M.; Li, X.; Hratchian, H. P.; Izmaylov, A. F.; Bloino, J.; Zheng, G.; Sonnenberg, J. L.; M. Hada, M. E.; Toyota, K.; Fukuda, R.; Hasegawa, J.; Ishida, M.; Nakajima, T.; Honda, Y.; Kitao, O.; Nakai, H.; Vreven, T.; Montgomery, J. A.; Jr., J. E. P.; Ogliaro, F.; Bearpark, M.; Heyd, J. J.; Brothers, E.; Kudin, K. N.; Staroverov, V. N.; Kobayashi, R.; Normand, J.; Raghavachari, K.; Rendell, A.; Burant, J. C.; Iyengar, S. S.; Tomasi, J.; Cossi, M.; Rega, N.; Millam, J. M.; Klene, M.; Knox, J. E.; J.B. Cross, V. B.; Adamo, C.; Jaramillo, J.; R. Gomperts; Stratmann, R. E.; Yazyev, O.; Austin, A. J.; Cammi, R.; Pomelli, C.; Ochterski, J. W.; Martin, R. L.; Morokuma, K.; Zakrzewski, V. G.; Voth, G. A.; Salvador, P.; Dannenberg, J. J.; Dapprich, S.; Daniels, A. D.; Farkas, O.; Foresman, J. B.; Ortiz, J. V.; Cioslowski, J.; Fox, D. J (2009) Gaussian 09. In revision A.01, Gaussian, Inc.: Wallingford, CT.